Henriette Frikke-Schmidt,[1,2] Thomas Å. Pedersen,[2] Christian Fledelius,[3] Grith S. Olsen,[2] Stephan D. Bouman,[3] Mark Fitch,[1] and Marc Hellerstein[1,4]

Treatment of Diabetic Rats With Insulin or a Synthetic Insulin Receptor Agonist Peptide Leads to Divergent Metabolic Responses

Diabetes 2015;64:1057–1066 | DOI: 10.2337/db14-0914

In addition to lowering of blood glucose, treatment with insulin also induces lipid synthesis and storage. Patients with type 2 diabetes often suffer from lipid-related comorbidities including dyslipidemia, obesity, and fatty liver disease. We examined here in two separate studies changes in lipid dynamics in Zucker diabetic fatty (ZDF) rats, in response to 7 days of treatment with either insulin or the insulin receptor agonist peptide S597. In concert with blood glucose normalization, the treated rats displayed large increases in hepatic de novo lipid synthesis and deposition of newly synthesized lipids in adipose tissue depots, accompanied by weight gain and expansion of adipose depots. In both treatment groups, heavy water labeling revealed that after 2 h (study A), de novo lipogenesis was responsible for 80% of newly stored hepatic triglyceride (TG)-palmitate, and after 5 days (study B), ~60% of newly deposited TG-palmitate in adipose tissues originated from this pathway. Interestingly, in both studies, treatment with the insulin mimetic peptide resulted in significantly lower blood TG levels, plasma TG production rates, and hepatic de novo synthesized fatty acid in plasma TG compared with insulin. There were no differences in plasma TG turnover (clearance rate) in response to either treatment, consistent with differential actions on the liver. These results show that in ZDF rats, treatment with a synthetic insulin-receptor-activating peptide or with insulin to lower blood glucose is accompanied by different effects on hepatic lipid anabolism and blood TG profiles.

A major target of interest when treating diabetic patients with insulin is lowering of blood glucose levels through activation of distinct signaling pathways downstream of the insulin receptor (1,2) in tissues, including muscle and adipose (1,2). Insulin-regulated metabolic signaling also results in alterations of lipid homeostasis. Expansion of adipose depots is known to occur in animals as well as in diabetic patients during insulin treatment (3,4). In insulin-resistant animals, there is evidence that the hepatic insulin receptor signaling pathways show differential responsiveness, such that the glucose-related pathways are more resistant than the ones orchestrating lipid responses (5). This results in the so-called insulin resistance triad, where two of the elements (hyperglycemia and hyperinsulinemia) reflect the reduced responsiveness to insulin on glucose metabolism, whereas the third element (hypertriglyceridemia) is believed to arise from the lipid-related pathways being less resistant and therefore excessively stimulated by the hyperinsulinemia (5). The hepatic metabolic response to insulin includes several processes: inhibition of endogenous glucose production (6), augmented glucose uptake (7), stimulation of de novo lipogenesis (DNL) (8), and inhibition of VLDL export

[1]Department of Nutritional Sciences and Toxicology, University of California, Berkeley, Berkeley, CA
[2]Department of Insulin Biology, Novo Nordisk, Maaloev, Denmark
[3]Department of Insulin Pharmacology, Novo Nordisk, Maaloev, Denmark
[4]KineMed, Inc., Emeryville, CA

Corresponding author: Marc Hellerstein, march@berkeley.edu.

Received 12 June 2014 and accepted 2 October 2014.

This article contains Supplementary Data online at http://diabetes.diabetesjournals.org/lookup/suppl/doi:10.2337/db14-0914/-/DC1.

(9). Insulin also induces fatty acid (FA) synthesis (10) and adipogenesis (11) in adipose tissues.

The main purpose of our experiments here was to assess lipid synthesis and storage in Zucker diabetic fatty (ZDF) rats in response to insulin treatment. We used heavy water labeling to quantify in situ to what extent these processes are affected by treatment with insulin or the synthetic insulin receptor agonist peptide S597.

Previous tissue culture experiments have shown that S597 differentially affected the mitogenic signaling downstream of the insulin receptor and the metabolic response (12,13). Since the classic metabolic responses such as inhibition of glucose production and induction of lipid synthesis diverge downstream from the insulin receptor and are differently affected in hepatic insulin resistance, our aim was to investigate if the intrinsic capability of S597 to differentially stimulate signaling also differently affected lipid and glucose metabolism in the whole animal.

RESEARCH DESIGN AND METHODS

Two independent studies were carried out, which we will call studies A and B. In study A, heavy water labeling took place for 2 h to measure acute effects on hepatic lipid synthesis. A group of lean heterozygous ZDF rats (lean vehicle group) was also included to reference if normoglycemia was reached with treatment. In study B, the labeling time was increased to 5 days to allow measurement of effects on lipid synthesis in adipose depots. In both studies, osmotic minipump treatment was for 7 days.

Animals

All animal experiments were approved by the University of California, Berkeley, Animal Care and Use Committee (study A) or the Danish Animal Experiment Inspectorate (study B). Twelve-week-old male ZDF or heterozygous lean control (lean vehicle) rats (Charles River Breeding Laboratories, Portage, MI [study A], or Sulzfeld, Germany [study B]) were fed the standard ZDF diet (Formulab 5008, LabDiet) ad libitum. They were stratified by blood glucose, body weight, and glycated hemoglobin (HbA_{1c}) values prior to randomization. In study B, the rats were additionally stratified for plasma triglyceride (TG) levels.

Treatment With Insulin or S597

At the age of 12 weeks, the rats had osmotic minipumps (Alzet, Model 2ML2, Cupertino, CA) inserted subcutaneously under isoflurane anesthesia. The pumps contained either vehicle (phosphate buffer; lean vehicle and ZDF vehicle), insulin Actrapid (0.2 mmol/L; Novo Nordisk, Bagsvaerd, DK; insulin), or S597 (0.4 mmol/L; S597). Analgesia was provided by intramuscular injection of 2 mg/kg meloxicam (Metacam, Boehringer Ingelheim, Ridgefield, CT) immediately prior to and every day for 3 days after implantation (study A) or by subcutaneous injection of 5 mg/kg carprofen (Rimadyl, Pfizer, Dundee, U.K.; study B). In study B, animals also received a single subcutaneous injection of enrofloxacin (Baytril, Bayer, Leverkusen, Germany). Throughout the treatment period, all rats were weighed daily. The pumps remained inserted for 7 days, after which the rats were killed by cardiac puncture under isoflurane anesthesia.

^2H_2O Labeling Protocol

Each rat received an intraperitoneal injection (35 mL/kg body weight) of 100% ^2H_2O (Cambridge Isotopes, Andover, MA) with 0.9% NaCl added for isotonicity. In study A, this was done 2 h prior to euthanization in nonfasted animals, whereas in study B, the injection was given 5 days prior to euthanization (i.e., 2 days after pump implantation). Sustained labeling took place by replacing drinking water with 8% ^2H_2O for a sustained body water enrichment of ~5% (14).

Blood Glucose and HbA_{1c} Quantification

Blood glucose was measured daily (study A, Contour Blood Glucose Meter, Bayer, Mishawaka, IN; study B, Biosen, EKF Diagnostic GmBH, Barleben, Germany).

HbA_{1c} was quantified in full blood on the day prior to pump implantation by tail vein bleed and at euthanization by cardiac puncture. In study A, kits from Chrystal Chem were used (catalog number 80300, Chrystal Chem, Downers Grove, IL). In study B, HbA_{1c} was measured by the use of standard laboratory procedures (Hitachi 912 automatic analyzer, Boehringer Mannheim, Germany).

Body Composition Measurement

In study B, body composition was measured in unanesthetized animals using quantitative magnetic resonance (QMR) to determine the body water content, from which relative body fat content is calculated (EchoMRI, Echo Medical Systems, Houston, TX).

Lipid Quantification in Liver and Plasma

All plasma lipids except free FAs (FFAs) were quantified in EDTA-stabilized plasma. FFA was measured in NaF-stabilized plasma.

Plasma TG levels in study A were quantified by Cayman Chemicals Triglyceride Colorimetric Kit (Cayman Chemicals, Ann Arbor, MI). Plasma TG levels in study B, hepatic TG levels in both studies, and cholesterol levels in both studies were all measured by standard laboratory procedures (Hitachi 912 automatic analyzer, Boehringer, Mannheim). Serum-free palmitate levels were quantified by gas chromatography-flame ionization detection as previously described (15) with heptadecanoic acid used as an internal standard. For the plasma samples that underwent thin layer chromatography prior to derivatization, heptadecanoic acid was replaced by tripentadecaonin to ensure that this internal standard followed the TG fraction on the thin layer chromatography plates.

Extraction, Derivatization, and Analysis of TG-Glycerol, Palmitate, Cholesterol, and Body Water

For analysis of tissue ~100 mg of tissue (the exact weight was known) or 150 μL of plasma was placed in 2:1 methanol: chloroform for overnight lipid extraction. Subsequently, the FAs were separated from glycerol by methylation with 5% methanolic acid by heating at 50°C for 1 h (16).

The FA methyl esters were extracted with hexane after the addition of water, whereas the phase containing free glycerol was dried down and converted to glycerol triacetate by incubation with 2:1 acetic anhydride:pyridine. The derivatized compounds were then run on gas chromatography–mass spectrometry, as described elsewhere (15).

Body water was isolated by overnight distillation of whole blood and processed for analysis of deuterium enrichment, as described previously (17).

Adipogenesis In Situ

Adipocytes from the distinct depots were isolated by collagenase digestion of the fresh tissue, as described elsewhere (18).

Isotopic enrichment of DNA was performed as previously described (19,20). Briefly, DNA was extracted following the protocol for samples with a low number of cells (21).

Calculations

Fractional Synthesis

The fraction of newly synthesized TG-glycerol and TG-palmitate formed during the ^2H_2O labeling period was assessed using a combinatorial model of polymerization biosynthesis, as described previously (14,17).

Corrected Fractional Synthesis

Measurement of fractional palmitate synthesis includes dilution by all unlabeled palmitate that was present in the adipose depots before the labeling experiment began. This causes an underestimation of the fractional contribution from de novo palmitate to the newly assembled and deposited TG. To correct for this underestimation, the ratio of fractional palmitate synthesis to fractional TG-glycerol synthesis is calculated, representing the fractional contribution from newly synthesized palmitates to the newly assembled and deposited TGs (17).

Absolute Rates of Palmitate and TG-Glycerol Synthesis

The absolute synthesis rate of palmitate/TG-glycerol in the tissues was calculated by multiplying the fractional synthesis rate by the amount of palmitate-TG present within each sample.

Fractional Glyceroneogenesis

From the enrichment of the glycerol moiety of TGs, the average number of deuterium incorporation sites within each molecule was calculated. As synthesis of glycerol via glyceroneogenesis and glycolysis, respectively, results in a different number of available sites for deuterium from deuterated water to become covalently incorporated, it is possible to calculate the fractional contributions from each pathway. A complete description of these calculations was presented elsewhere (14).

Statistical Analysis

Statistical significance was tested by *t* test, one-way ANOVA, or two-way ANOVA as appropriate (the two latter followed by Bonferroni pairwise comparisons). The type of test used is given with each figure. Prior to statistical analysis the ROUT outlier test with Q = 1% was applied to all data sets to exclude potential outliers. Data sets that did not meet the requirements for equal variances were log or square root transformed prior to analysis. $P < 0.05$ was considered significant for all tests. All statistical analysis were performed in Prism (version 5, GraphPad Software Inc., La Jolla, CA).

RESULTS

Two similar but independent studies were carried out in order to follow lipid dynamics: study A and study B. In study A, heavy water labeling took place for 2 h to follow hepatic lipid synthesis and a lean control (lean vehicle) group was included. In study B, the labeling time was increased to 5 days to allow measurement of lipid synthesis in the adipose depots.

Blood Glucose Lowering by Insulin and S597

In both studies, diabetic ZDF rats had osmotic minipumps implanted releasing either phosphate buffer (lean vehicle and ZDF vehicle), insulin, or S597. The doses chosen resulted in blood glucose levels that ended close to the levels in the nondiabetic lean vehicle group (Fig. 1*A*). The blood-glucose lowering happened slightly more slowly with S597 than with insulin. During the heavy water labeling period, however, the response was similar (Fig. 1*A* and *B*). These findings were supported by the glucose area under the curve as well as the HbA_{1c} values (data not shown) both of which were significantly lower when compared with the ZDF vehicle group but did not differ between insulin and S597 treatments.

Body and Tissue Weight

In both studies, the insulin- or S597-treated animals gained more body weight than the vehicle treated ZDF rats (Supplementary Fig. 1*A* and *B*). Food intake, however, was not significantly different between groups (data not shown). QMR scans in study B showed that the insulin- or S597-treated rats gained significantly more fat mass than the ZDF vehicle group (Table 1), with a nonsignificant trend for the S597 group to gain less fat than the insulin group. The same pattern was observed for the liver weights (Fig. 2*A*), where the untreated rats had significantly smaller livers than the treated groups. Additionally, S597 treatment resulted in slightly less expansion of liver mass than regular insulin. The subcutaneous adipose depot was highly responsive to treatment with a 25% increase in mass when comparing to the ZDF vehicle group (Fig. 2*B*). Of the remaining adipose depots, the epididymal and perirenal fat pads increased slightly with insulin treatment, whereas the mesenteric depot was unaffected (Supplementary Fig. 2*A–C*).

Lipid Levels in Plasma, Liver, and Adipose Tissues

Total plasma and liver TG and palmitate levels where assessed at the end of both studies (Table 2). TG and palmitate both increased in plasma with insulin treatment, albeit this was significant only in study B. A very

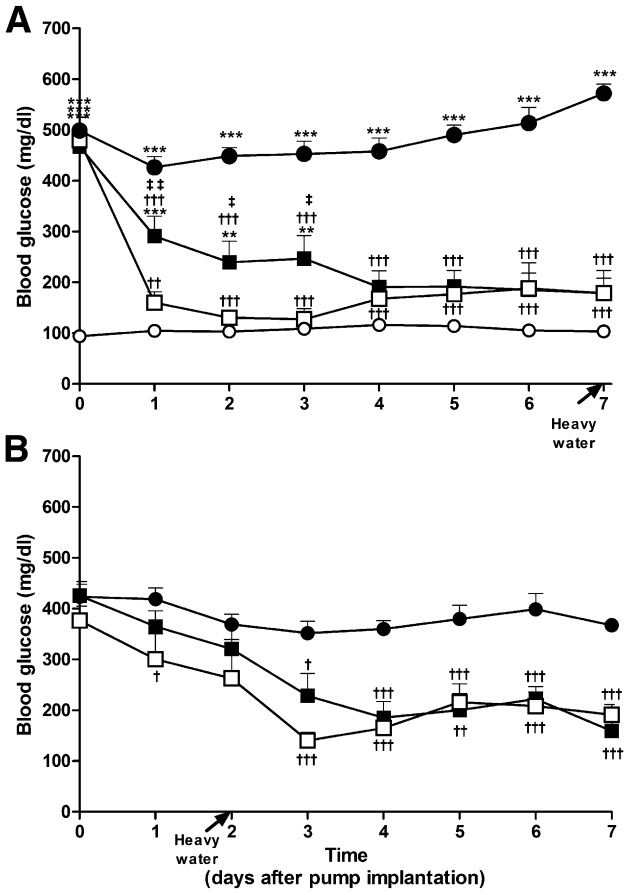

Figure 1—Blood glucose. Blood glucose concentrations after subcutaneous implantation of osmotic minipumps containing buffer in the lean vehicle group (white circles) and the ZDF vehicle group (black circles), 0.2 mmol/L of insulin in ZDF rats (white squares) or 0.4 mmol/L of S597 in ZDF rats (black squares). *A*: The results from study A where a lean control group (lean vehicle) was included. *B*: The glucose levels from study B. The time for heavy water injection is depicted by an arrow on the *x*-axis. $^{**}P < 0.01$ and $^{***}P < 0.001$ as compared with lean vehicle; $\dagger P < 0.05$, $\dagger\dagger P < 0.01$, and $\dagger\dagger\dagger P < 0.001$ as compared with ZDF vehicle; $\ddagger P < 0.05$ and $\ddagger\ddagger P < 0.01$ as compared with insulin (Bonferroni posttests upon two-way ANOVA). Error bars are SEM (in some groups, error bars are not visible due to their small value).

Table 1—Whole body composition by QMR scan

	Pretreatment fat mass (g)	Posttreatment fat mass (g)	ΔFat mass (g)
ZDF vehicle	85.3 ± 1.0	85.7 ± 1.6	0.4 ± 1.8
Insulin	83.9 ± 1.9	100.3 ± 2.4***	16.5 ± 1.6***
S597	82.7 ± 1.9	94.4 ± 2.3*	11.7 ± 1.1***

Rats from study B were scanned on the day prior to treatment and again on the day prior to euthanization. Values are expressed as mean ± SEM. $^{*}P < 0.05$ as compared with ZDF vehicle (one-way ANOVA with Bonferroni posttests). $^{***}P < 0.001$ as compared with ZDF vehicle (one-way ANOVA with Bonferroni posttests).

prominent reduction in plasma TG levels, however, was observed with S597 treatment in both studies. The levels were more than halved as compared with insulin and were decreased even below the levels found in the vehicle-treated ZDF rats. The same pattern from S597 treatment was observed with plasma palmitate. In contrast, plasma FFAs were reduced with both insulin and S597 treatment, and in study A, a slight increase in plasma cholesterol was found. The estimated TG content of the subcutaneous adipose depot reflected increased adipose mass and was highly responsive to treatment. The palmitate levels also showed a nonsignificant trend toward increasing with insulin or S597 treatment. Of the remaining adipose depots (Supplementary Table 1), the epididymal and perirenal fat pads both increased in mass with insulin and S597 treatment, whereas the mesenteric content of palmitate and TG did not change.

Hepatic and Adipose DNL

In all tissues studied, fractional palmitate synthesis was greatly induced by insulin or S597 treatment, with approximately threefold increases in fractional synthesis in liver and plasma and a 10-fold increase in the subcutaneous adipose depot (Fig. 3*A–C*). No differences between the insulin and S597 groups were observed for fractional palmitate synthesis in any tissue studied. The corrected fractional synthesis (Fig. 3*D–F*) showed that in tissues from the vehicle-treated ZDF rats, only ~20% of the palmitate present in new TG molecules was de novo synthesized, whereas with treatment, this fraction increased to ~80% (liver) and even higher (plasma), reflecting almost exclusively a DNL contribution to palmitate for new TG assembly. Interestingly, when compared with insulin, S597 gave rise to slightly but significantly higher corrected fractional synthesis contribution in plasma, yet when accounting for the total amounts of TG-palmitate present in plasma, the net result was a halving of newly synthesized palmitate (Fig. 3*H*). The massive increase in fractional synthesis in the subcutaneous depot was also observed in the remaining adipose depots (see Supplementary Fig. 3), although fractional synthesis, corrected fractional synthesis, and absolute palmitate synthesis were all nonsignificantly lower with S597 treatment.

Hepatic and Adipose TG-Glycerol Synthesis (All-Source TG Synthesis)

TG-glycerol synthesis rate measures new TG formation, irrespective of the source of the FAs. In contrast to what was observed with palmitate synthesis, the fractional synthesis values for TG-glycerol in the liver and plasma over 2 h (Fig. 4*A* and *B*) were affected only slightly by insulin or S597 treatment. This parameter reflects replacement rate or half-life of TG in the compartment and remained relatively constant at ~20% in the liver and 80% in plasma. There was only a small, though significant, increase with insulin treatment as compared with ZDF vehicle in the liver. In the adipose depots, in contrast, there was a significant increase in fractional

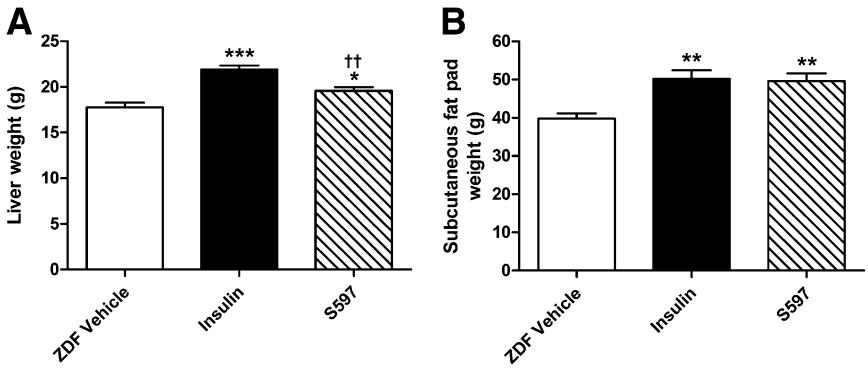

Figure 2—Weight of liver and subcutaneous adipose depot. In study B, the liver and subcutaneous adipose depot were carefully dissected and weighed. *P < 0.05, **P < 0.01, and ***P < 0.001 as compared with ZDF vehicle; ††P < 0.01 as compared with insulin (one-way ANOVA with Bonferroni posttests). Error bars are SEM.

TG-glycerol synthesis over 5 days with insulin or S597 treatment. Interestingly, fractional TG-glycerol synthesis was slightly but consistently and significantly higher in the S597-treated group as compared with the insulin group in all adipose depots (Fig. 4*C* for subcutaneous depot and Supplementary Fig. 4*A–C* for the epididymal, perirenal, and mesenteric depots). Calculation of the absolute amounts of newly assembled TG (Fig. 4*D* and *E* and Table 2) revealed that the amounts of new TG in plasma were more than halved with S597 treatment as compared with both the insulin and vehicle groups. In all adipose depots, significantly more lipids were accumulated in the form of TG in response to insulin or S597 treatment (Fig. 4*I* for the subcutaneous depot and Supplementary Fig. 4*D–F* for the epididymal, perirenal, and mesenteric depots).

Metabolic Source of Hepatic and Adipose TG-Glycerol Synthesis

The glycerol used for TG assembly can originate from two distinct biosynthetic pathways: glyceroneogenesis or glycolysis. The fraction of new glycerol being synthesized via the glyceroneogenic pathways is given in Fig. 4*G–I*. In liver and plasma, more than 70% of the new glycerol for TG came from glyceroneogenesis, whereas only up to 30% originated from this pathway in the adipose tissue (the same was observed in the remaining adipose depots; data not shown). Treatment affected the tissue specific biosynthetic origin differently. In liver and plasma, slightly more TG-glycerol originated from glycolysis in the insulin- and S597-treated groups as compared with the vehicle-treated ZDF group, whereas the percentage of contribution from this pathway decreased slightly but

Table 2—Lipid content of liver, plasma, and the subcutaneous adipose depot

	Study A			Study B		
	ZDF controls	Insulin	S597	ZDF controls	Insulin	S597
Liver						
TG (mg/liver)	660 ± 100	805 ± 115	719 ± 126	384 ± 35	416 ± 43	337 ± 32
Palmitate (mg/liver)	153 ± 15	204 ± 9	190 ± 27	159 ± 9	204 ± 9*	177 ± 15
Cholesterol (mg/liver)	50.3 ± 2.9	53.6 ± 2.8	47.1 ± 4.3	63.7 ± 2.3	68.3 ± 3.7	57.9 ± 3.2
Plasma						
TG (mg/dL)	541 ± 68	637 ± 122	275 ± 42*,††	624 ± 58	964 ± 54***	462 ± 47†††
Palmitate (mg/dL)	12.4 ± 1.7	17.3 ± 3.4	7.1 ± 1.0††	20.8 ± 1.7	34.0 ± 2.8***	19.6 ± 1.9†††
FFA (mg/dL)	N/A	N/A	N/A	6.41 ± 1.19	3.40 ± 0.28	2.22 ± 0.26*
Cholesterol (mg/dL)	177 ± 4	199 ± 8*	225 ± 5***,†	146 ± 7	132 ± 4	147 ± 7
Subcutaneous adipose depot						
TG (g/depot)	N/A	N/A	N/A	31.9 ± 3.0	40.1 ± 5.2**	39.7 ± 4.5**
Palmitate (g/depot)	N/A	N/A	N/A	2.27 ± 0.20	2.60 ± 0.38	2.56 ± 0.33

TG, palmitate, and cholesterol were all quantified in the liver. TG, palmitate, FFA, and cholesterol were quantified in plasma. Palmitate was quantified and TG content was estimated based on fat pad mass in the subcutaneous adipose depot. Values are expressed as mean ± SEM. N/A, not available. *P < 0.05 as compared with ZDF controls (one-way ANOVA with Bonferroni posttests). **P < 0.01 as compared with ZDF controls (one-way ANOVA with Bonferroni posttests). ***P < 0.001 as compared with ZDF controls (one-way ANOVA with Bonferroni posttests). †P < 0.05 as compared with insulin (one-way ANOVA with Bonferroni posttests). ††P < 0.01 as compared with insulin (one-way ANOVA with Bonferroni posttests). †††P < 0.001 as compared with insulin (one-way ANOVA with Bonferroni posttests).

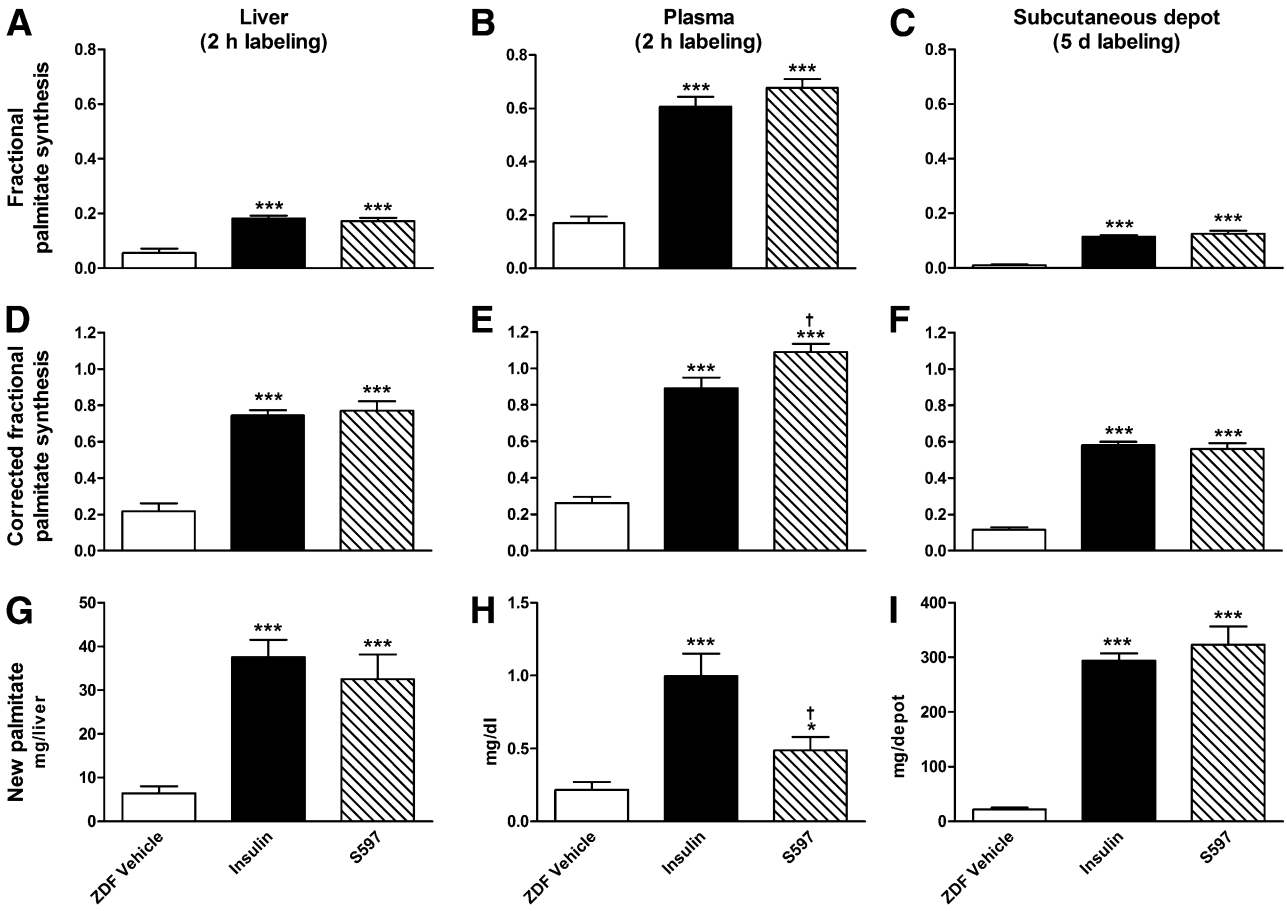

Figure 3— Palmitate synthesis. Fractional palmitate synthesis in liver, plasma, and the subcutaneous adipose depot is given in *A*, *B*, and *C*. The corrected fractional palmitate synthesis (for liver [*D*], for plasma [*E*], and for the subcutaneous adipose depot [*F*]) is a measure of how large a fraction of palmitate in only the newly formed TGs is de novo synthesized. Liver (*G*), plasma (*H*), and subcutaneous adipose depot (*I*) are the quantified amounts of new palmitate present within each tissue. $^{*}P < 0.05$ and $^{***}P < 0.001$ as compared with ZDF vehicle; †$P <$ 0.05 as compared with insulin (one-way ANOVA with Bonferroni posttests). Error bars are SEM.

significantly in the subcutaneous adipose depot after treatment.

In summary, these TG-glycerol synthesis results indicate that storage of newly assembled TG took place in the adipose depots upon insulin treatment, whereas TG synthesis in liver and plasma remained relatively unaffected. With S597 treatment, however, the amount of new TG was greatly reduced in plasma, and in all adipose depots, the fractional TG-glycerol synthesis rates were slightly but significantly higher than with insulin treatment. This could indicate a small improvement in TG uptake in the adipose tissues that was more sensitive than net TG accumulation, which did not reflect any difference between treatments.

Adipogenesis In Situ

In situ adipogenesis was investigated by quantifying the fractional amount of newly replicated DNA in freshly isolated adipocytes (Fig. 5*A* and *B*). In the subcutaneous depot, insulin treatment caused a significant upregulation of DNA synthesis in the adipocytes, whereas S597 did not cause any significant changes in fractional DNA synthesis. In the epididymal depot, however, the adipogenic response to S597 treatment was more pronounced, with a doubling of fractional DNA synthesis as compared with the ZDF vehicle group, while insulin treatment had no significant effect.

DISCUSSION

In the current studies, we set out to investigate the effects of insulin on lipid dynamics in the diabetic, insulin resistant ZDF rat model. Additionally, we tested whether the intrinsic capability of S597 to stimulate signaling downstream of the insulin receptor was differentiated from the effects of insulin at equal glucose-reducing doses in these animals.

Treatment of ZDF rats with the insulin receptor agonist peptide S597 by mini–osmotic pump resulted in significantly lower plasma TG levels than treatment with insulin, despite no significant differences in glycemic control, in both of the 7-day treatment studies that we carried out. In one of the studies, insulin treatment significantly increased the already elevated plasma TG levels in ZDF rats, while S597 had no effect on TGs. In the other study, S597 significantly lowered plasma TGs,

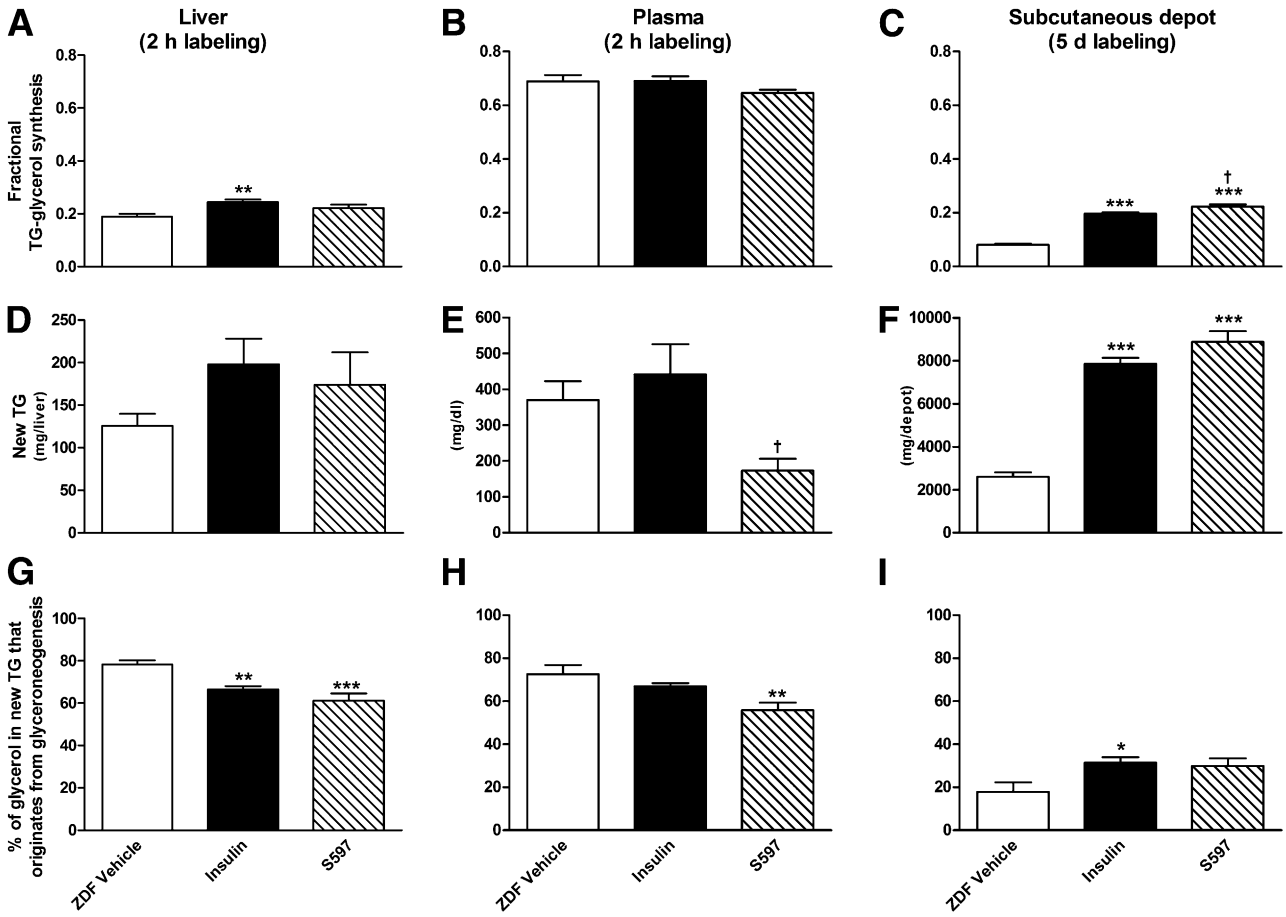

Figure 4—TG-glycerol synthesis and biosynthetic origin in liver, plasma, and subcutaneous adipose depot. Liver (*A*), plasma (*B*), and subcutaneous adipose depot (*C*) are measures of fractional TG-glycerol synthesis with 2 h (liver and plasma) and 5 days (adipose tissue) of heavy water labeling. The absolute quantified levels of TGs containing a new glycerol moiety are depicted in liver (*D*), plasma (*E*), and subcutaneous adipose depot (*F*). The biosynthetic origin of all new TG-glycerol, e.g., how large a percentage of glycerol that originates from glyceroneogenesis versus glycolysis is given in liver (*G*), plasma (*H*), and subcutaneous adipose depot (*I*), respectively. *$P < 0.05$, **$P < 0.01$, and ***$P < 0.001$ as compared with ZDF vehicle; †$P < 0.05$ as compared with the insulin group (one-way ANOVA with Bonferroni posttests). Error bars are SEM.

while insulin did not have a significant effect. The differential plasma TG response was associated with a significantly lower plasma TG production rate and significantly less stimulation of hepatic de novo synthesized FA input into plasma TG in response to S597. Importantly, there were no differences in plasma TG replacement (clearance rate) in response to either treatment, consistent with the differential effect acting through liver metabolism rather than peripheral clearance of TG.

The biosynthetic signature of blood lipids reflected the findings in liver, supporting the source of blood lipids sampled as deriving primarily from liver rather than adipose tissue or diet. Contribution from the glyceroneogenic pathway to TG-glycerol was lower in blood after treatment by either agent compared with vehicle treatment with very similar values and effects of treatment in the liver (vehicle-treated exhibited ~80% from glyceroneogenesis, and treatment with either agent exhibited ~60% in both compartments). In contrast, adipose tissue TG-glycerol was derived only ~20% from glyceroneogenesis and was modestly increased by treatment with insulin or S597. The fraction of newly assembled TG-palmitate in plasma that derived from de novo synthesis was 80–100% after treatment with insulin or S597, compared with ~20% in vehicle-treated animals, again closely paralleling values in liver (80 and 20%, respectively) but different from adipose depots (~50 and 20%, respectively). Plasma TG clearly reflected, and likely derived from, lipids in the liver.

Moreover, liver weight was increased less by S597 than by insulin and these results indicate less stimulation of hepatic anabolic pathways by S597 compared with insulin.

Taken together, these findings strongly support the conclusion that both S597 and insulin treatment have potent effects on lipid biosynthesis in the liver of diabetic rats but that there are significant differences in the rate of TG release into the bloodstream. Biosynthetic origins of the glycerol and FA moieties of liver TG were altered by treatment with both insulin and S597, and these alterations were observed in plasma TG, but the rate of blood TG production was dramatically lower with S597

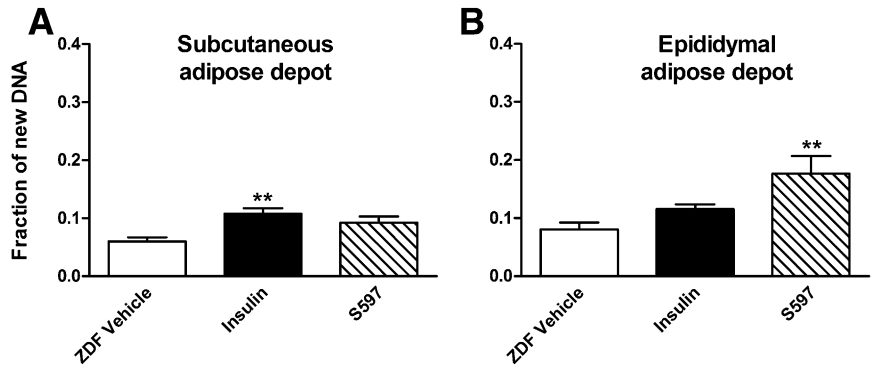

Figure 5—Adipogenesis in situ. Adipocyte and preadipocyte proliferation (adipogenesis) in the subcutaneous and epididymal depots, respectively, measured as fraction of DNA that has been newly synthesized within the 5 days of heavy water labeling. $^{**}P < 0.01$ as compared with ZDF vehicle (one-way ANOVA with Bonferroni posttests). Error bars are SEM.

treatment. The lower production rate explained the more than 50% reduced blood TG concentrations with S597 treatment, as there was no effect of either agent on clearance (half-life) of plasma TG. These observations are all consistent with S597 treatment resulting in less secretory input from hepatic lipogenic pathways into plasma TG compared with insulin treatment.

In contrast, adipose lipogenesis was not differentially stimulated by S597 and insulin. Storage of newly synthesized palmitate and TG in adipose, as well as TG content, were all markedly and similarly stimulated by the two agents.

Can these apparent differential actions be explained by different glucose-lowering effects of the two treatment regimens? Our studies were designed to achieve equal glucose lowering by S597 and insulin in order to avoid any confounding of potential insulin effects on different lipid pathways. The treatments both significantly reduced HbA_{1c} and glucose concentrations from pretreatment levels, without any significant differences between the two agents.

Plasma glucose concentrations did fall more rapidly with insulin treatment, however, and HbA_{1c} values were nonsignificantly reduced more by insulin while body weights were nonsignificantly higher compared with S597. The possibility that subtle differences in net insulin effect could explain the divergent hepatic lipid anabolic responses by S597 as compared with insulin therefore seems unlikely, although it cannot be completely excluded. Of note, plasma glucose levels were identical in the two treatment arms at the start time of the 2-h labeling study (study A), so divergent acute effects cannot be explained even by subtle differences in glycemic control.

What might then explain the divergent metabolic response exerted by S597 compared with insulin? Previous work with insulin receptor ligands and their interaction with the receptor suggests that there are several binding characteristics that have the potential to alter downstream signaling, e.g., residence time of the ligand on the receptor, the ability of the ligand to induce more or less phosphorylation at distinct phosphorylation sites, or how internalization of the receptor/ligand complex takes place (1,13). Regarding S597 in particular, it seems to cause phosphorylation of the same number of insulin receptors but to a lower degree, and also it has been found that S597 remained associated with the receptor for longer periods of time than native insulin (13). It has to be kept in mind, however, that these changes were observed in tissue culture systems, and it is unknown whether such changes take place and are of significance in whole animals. It is worth noting that ZDF rats exhibited remarkably active rates of DNL with either treatment. Insulin and S597 treatments each significantly stimulated adipose DNL in ZDF rats so that after 5 days of labeling, ~60% of newly deposited TG-palmitate in adipose tissue came from the de novo lipogenic pathway in both treatment groups. Moreover, after 2 h of labeling, essentially 100% of newly secreted plasma TG-palmitate and 80% of newly stored hepatic TG-palmitate came from the de novo lipogenic pathway in each group. Endogenous synthesis of FAs is clearly a very active pathway in ZDF rats exposed to insulin receptor agonists. This marked induction of de novo lipid synthesis might partly explain why our studies showed increased TG levels in the plasma upon insulin therapy (this effect was highly significant in study 2) (see Table 2), which is otherwise reported to improve hypertriglyceridemia in diabetic subjects in the clinic due to better glycemic control (22). We did not measure the effects of insulin or S597 treatment on plasma apolipoprotein B levels or production rates, which could have implications for atherogenesis. The effects on TG-rich particle numbers and production will be an interesting area for future inquiry.

Insulin is also well-known to be a potent stimulator of adipogenesis in vitro (23,24). To the best of our knowledge, we here show for the first time that insulin treatment of diabetic animals can increase adipogenesis in situ. Interestingly, it was the epididymal depot only that displayed increased adipogenesis in response to S597

treatment, both when compared with the ZDF vehicle group and to insulin treatment. It has previously been shown that in human diabetic subjects, the subcutaneous depot displays less adipogenic potential when compared with visceral depots (25), which may partly explain this observation. Taken together with the substantial expansion of the subcutaneous depot, in particular, with insulin and S597 treatment, these adipogenesis results suggest that the subcutaneous depot responded to S597 treatment by expanding the already existing adipocytes, whereas the epididymal depot was also able to produce more adipocytes to incorporate the extra TG. Additional experiments with estimation of adipocyte size would be needed to address this hypothesis.

Finally, it is of interest to note than kinetic measurements were able to detect effects of insulin-receptor-activating peptides or insulin on adipose lipids where traditional nonkinetics metrics could not detect effects. In ZDF rats, the content of palmitate in each fat pad was ~300–500 mg (Supplementary Fig. 3). Treatment for 7 days did not generally cause measurable increases. In contrast, the kinetic measurement (fractional synthesis from the de novo lipogenic pathway) showed consistent and striking increases, and the total amount of newly synthesized palmitate was even more strikingly elevated by treatment. The numbers involved may help explain the different sensitivity of kinetic versus static techniques. The fractional contribution over 7 days from de novo palmitate synthesis was 5–10%, representing ~20–40 mg new palmitate out of 300–500 mg total palmitate. It is easy to see how pool size measurements might not be able to detect these changes, whereas mass spectrometric measurements can sensitively distinguish between 5 and 10% values.

In summary, pathways of hepatic TG assembly (glyceroneogenesis) and TG secretion (de novo FA and TG release into plasma) were significantly different between the peptide receptor agonist S597 and insulin itself, despite similar effects on adipose TG metabolism. These results reveal differential effects of insulin and the insulin receptor agonist S597 on lipid anabolic pathways in liver but not in adipose tissue. Subtle differences in glycemia are unlikely to explain these tissue-specific differences in lipogenesis. The capacity to modulate hepatic lipogenic pathways differentially with insulin-receptor-activating peptides could have important therapeutic applications.

Acknowledgments. The authors thank Simply Floracruz (University of California, Berkeley), Mersedeh Hakimzadeh (University of California, Berkeley), Vibeke Ladas (Novo Nordisk), Christina Zachodnik (Novo Nordisk), Jesper Damgaard (Novo Nordisk), and Helle Nygaard (Novo Nordisk) for their assistance with the animals; Lauge Schäffer (Novo Nordisk) and Kasper Huus (Novo Nordisk) for synthesis and formulation of S597; as well as Kirsten Vestergaard (Novo Nordisk), Rikke Ingvorsen (Novo Nordisk), and Gitte-Mai Nelander (Novo Nordisk) for their outstanding technical support concerning the tissue analysis.

Duality of Interest. This study was funded by Novo Nordisk, through which T.Å.P., C.F., G.S.O., and S.D.B. are employees and stakeholders. The insulin and the peptide used for the experiments were provided by Novo Nordisk as well. This does not alter our adherence to all the *Diabetes* policies on sharing data and materials. All Intellectual Property Rights of the current study are owned by the University of California, Berkeley, and there has been no compromise of the objectivity or validity of the data in the article. T.Å.P., C.F., G.S.O., and S.D.B. are employees and stakeholders of Novo Nordisk, which owns the peptide receptor agonist S597. H.F.-S. was partly employed by Novo Nordisk during some of this work and was included in the contract placing all intellectual property with the University of California, Berkeley. She was no longer affiliated with Novo Nordisk at the time of manuscript submission and she has never been a Novo Nordisk stakeholder. No other potential conflicts of interest relevant to this article were reported.

Author Contributions. H.F.-S. designed the study; performed the experiments; analyzed collected samples; interpreted results of experiments; prepared figures; drafted the manuscript; and edited, revised, and approved the final version of the manuscript. T.Å.P., C.F., G.S.O., S.D.B., and M.H. designed the study; interpreted results of experiments; and edited, revised, and approved the final version of the manuscript. M.F. analyzed collected samples. M.H. is the guarantor of this work and, as such, had full access to all the data in the study and takes responsibility for the integrity of the data and the accuracy of the data analysis.

References

1. Jensen M, De Meyts P. Molecular mechanisms of differential intracellular signaling from the insulin receptor. Vitam Horm 2009;80:51–75
2. Faerch K, Brøns C, Alibegovic AC, Vaag A. The disposition index: adjustment for peripheral vs. hepatic insulin sensitivity? J Physiol 2010;588:759–764
3. Heller S. Weight gain during insulin therapy in patients with type 2 diabetes mellitus. Diabetes Res Clin Pract 2004;65(Suppl. 1):S23–S27
4. Frikke-Schmidt H, Pedersen TÅ, Fledelius C, Olsen GS, Hellerstein M. Adipose weight gain during chronic insulin treatment of mice results from changes in lipid storage without affecting de novo synthesis of palmitate. PLoS ONE 2013; 8:e76060DOI: 10.1371/journal.pone.0076060
5. Brown MS, Goldstein JL. Selective versus total insulin resistance: a pathogenic paradox. Cell Metab 2008;7:95–96
6. Chiasson JL, Liljenquist JE, Finger FE, Lacy WW. Differential sensitivity of glycogenolysis and gluconeogenesis to insulin infusions in dogs. Diabetes 1976; 25:283–291
7. Steele R, Bishop JS, Dunn A, Altszuler N, Rathbeb I, Debodo RC. Inhibition by insulin of hepatic glucose production in the normal dog. Am J Physiol 1965; 208:301–306
8. Li S, Brown MS, Goldstein JL. Bifurcation of insulin signaling pathway in rat liver: mTORC1 required for stimulation of lipogenesis, but not inhibition of gluconeogenesis. Proc Natl Acad Sci U S A 2010;107:3441–3446
9. Sørensen LP, Andersen IR, Søndergaard E, et al. Basal and insulin mediated VLDL-triglyceride kinetics in type 2 diabetic men. Diabetes 2011;60:88–96
10. Dimitriadis G, Mitrou P, Lambadiari V, Maratou E, Raptis SA. Insulin effects in muscle and adipose tissue. Diabetes Res Clin Pract 2011;93(Suppl. 1):S52–S59
11. Sorisky A. From preadipocyte to adipocyte: differentiation-directed signals of insulin from the cell surface to the nucleus. Crit Rev Clin Lab Sci 1999;36:1–34
12. Jensen M, Palsgaard J, Borup R, de Meyts P, Schäffer L. Activation of the insulin receptor (IR) by insulin and a synthetic peptide has different effects on gene expression in IR-transfected L6 myoblasts. Biochem J 2008;412:435–445
13. Jensen M, Hansen B, De Meyts P, Schäffer L, Ursø B. Activation of the insulin receptor by insulin and a synthetic peptide leads to divergent metabolic and mitogenic signaling and responses. J Biol Chem 2007;282:35179–35186
14. Turner SM, Murphy EJ, Neese RA, et al. Measurement of TG synthesis and turnover in vivo by 2H2O incorporation into the glycerol moiety and application of MIDA. Am J Physiol Endocrinol Metab 2003;285:E790–E803
15. Hellerstein MK, Neese RA, Schwarz JM. Model for measuring absolute rates of hepatic de novo lipogenesis and reesterification of free fatty acids. Am J Physiol 1993;265:E814–E820

16. Pouteau E, Beysen C, Saad N, Turner S. Dynamics of adipose tissue development by 2H2O labeling. Methods Mol Biol 2009;579:337–358
17. Strawford A, Antelo F, Christiansen M, Hellerstein MK. Adipose tissue triglyceride turnover, de novo lipogenesis, and cell proliferation in humans measured with 2H2O. Am J Physiol Endocrinol Metab 2004;286:E577–E588
18. Whitesell RR, Gliemann J. Kinetic parameters of transport of 3-O-methylglucose and glucose in adipocytes. J Biol Chem 1979;254:5276–5283
19. Tchoukalova YD, Fitch M, Rogers PM, et al. In vivo adipogenesis in rats measured by cell kinetics in adipocytes and plastic-adherent stroma-vascular cells in response to high-fat diet and thiazolidinedione. Diabetes 2012;61:137–144
20. Neese RA, Misell LM, Turner S, et al. Measurement in vivo of proliferation rates of slow turnover cells by 2H2O labeling of the deoxyribose moiety of DNA. Proc Natl Acad Sci U S A 2002;99:15345–15350
21. Busch R, Neese RA, Awada M, Hayes GM, Hellerstein MK. Measurement of cell proliferation by heavy water labeling. Nat Protoc 2007;2:3045–3057
22. Haffner SM. Management of dyslipidemia in adults with diabetes. Diabetes Care 1998;21:160–178
23. Gamou S, Shimizu N. Adipocyte differentiation of 3T3-L1 cells in serum-free hormone-supplemented media: effects of insulin and dihydroteleocidin B. Cell Struct Funct 1986;11:21–30
24. García-Escobar E, Rodríguez-Pacheco F, Haro-Mora JJ, et al. Effect of insulin analogues on 3t3-l1 adipogenesis and lipolysis. Eur J Clin Invest 2011;41:979–986
25. Patel P, Abate N. Role of subcutaneous adipose tissue in the pathogenesis of insulin resistance. J Obes 2013;2013:489187